

TYPE-III RESOLVER-TO-DIGITAL CONVERTER USING SYNCHRONOUS DEMODULATION

RAYMUNDO C. GARCÍA, JOÃO O. P. PINTO, EDSON A. BATISTA, MARCIO A. S. GRASSI

*Pós Graduação em Engenharia Elétrica, Universidade Federal de Mato Grosso do Sul
Cidade Universitária s/n, Campo Grande – MS, CEP 79070-900*

*E-mails: rcordeiro@gmail.com, joaonofre@gmail.com, edson.batista@ufms.br,
marciograssi14@gmail.com*

Abstract— Resolver is an angular position sensor widely used in applications such as electric/hybrid vehicles, CNCs, antennas and robotics. However, the estimation of the angular position from resolver outputs is more difficult than the analysis of encoder signals, and it is still an open question. Most algorithms proposed in literature are based on type-I or type-II angle tracking observers. Recently, a type-III observer was proposed, but it requires a high sampling frequency. This paper explores the use of synchronous demodulation of the resolver outputs to simplify the implementation of a type-III angle tracking observer. The resolver outputs are sampled at the peaks and valleys of the excitation resolver signal, being easy to get sine and cosine of the angular position. The proposed approach reduces the computational cost and the required sampling frequency to implement the type-III observer. Simulation and experimental results proves the accuracy of the proposed approach.

Keywords— Angle tracking observer, DSP, resolver, resolver-to-digital converter, type-III observer.

Resumo— O resolver é um sensor amplamente utilizado em aplicações como veículos elétricos/híbridos, CNC, antenas e robótica. Porém, a estimação da posição angular a partir das saídas do sensor é mais complexa que analisar os sinais de um encoder, sendo ainda uma questão aberta. Muitos algoritmos propostos estão baseados em estimadores de ângulo tipo-I e tipo-II. Recentemente, um observador tipo-III foi proposto, mas precisa de uma alta taxa de amostragem. O presente artigo explora o uso da demodulação síncrona para simplificar a implementação do observador de rastreamento de ângulo tipo-III. As saídas do resolver são amostradas quando o sinal de excitação do resolver atinge seus valores máximos e mínimos, sendo simples obter o seno e cosseno da posição angular. O sistema proposto reduz o custo computacional e a frequência de amostragem necessários para implementar o observador tipo-III. Resultados de simulação e experimentais demonstram a exatidão o observador proposto.

Palavras-chave— Observador de rastreamento de ângulo, DSP, resolver, conversor resolver a digital, observador tipo-III.

1 Introduction

Applications such as CNC, aircrafts, hybrid/electric vehicles and robotics have to work under harsh conditions: high temperature, shocks and vibrations (Lee et al., 1992; Zhang et al., 2015; Staebler and Verma, 2017). In these kinds of applications, even with the development of sensorless algorithms, angular position sensors are still used to guarantee the robustness and reliability of the drives, while sensorless techniques are used as backup systems in case of sensor failure (Cordero et al., 2017).

Resolver is widely used as absolute angular position sensor for harsh environments due to it has more precision, long operational lifetime and robustness than encoders (Kaewjinda and Konghirun, 2006). For example, resolvers resist shocks up to 200G, vibrations up 40G and temperatures up to 220°C, while most encoders only resists shocks up to 100G, vibrations up to 10G, and temperatures below 120°C (Jin et al, 2015).

The resolver outputs are amplitude-modulated signals which give information about the sine and cosine of the angular position. Hence, the decoding of the resolver signals is more difficult than the position sensing using encoders. Observers called resolver-to-digital converters (RDCs) are used to get the

angular position and speed from resolver signals (Staebler and Verma, 2017). Nowadays, most drives use software-based RDCs which are implemented in the same digital processor where the control system is implemented, instead of using an additional external hardware (Caruso et. al., 2016). Due to the resolver signal outputs are analog signals, the resolution of the angle measurement using resolver depends on the RDC system. Usually, RDCs has a resolution of 10, 12, 14 or 16 bits (Szymczak et. al., 2014).

Most software-based RDCs are based on type-I or type-II closed-loop observers (Idkhajine et. al., 2012; Bergas-Jané et. al., 2012; Qamar et. al., 2015; Wang et. al., 2015; Caruso et. al., 2016). Some of them use oversampling of the resolver signals. In (Bergas-Jané et. al., 2012), it is used a sampling frequency of 288 kHz. On the other hand, some RDCs are based in undersampling demodulation (Idkhajine, et. al., 2009): the resolver outputs are sampled at the peaks and/or valleys of the resolver excitation signal. This method requires low sampling ratio and it is simpler to implement. In (Cordero et. al., 2017), it is proposed a type-III angle tracking observer (ATO) which can track the angular position even for constant acceleration. However, that approach also uses oversampling technique: it is used a sampling frequency of 50 kHz, and the excitation resolver signal multiplies the resolver output signals.

This paper explores the use of synchronous demodulation of the resolver outputs in order to reduce computational complexity of a type-III ATO. The resolver outputs are demodulated by sampling them at the peaks and valleys of the excitation resolver signal. These demodulated signals are used by the ATO to estimate the angular position. The proposed approach reduces the required sampling ratio and the computational cost of the RDC, which is an important characteristic when an algorithm is implemented in a DSP or FPGA. Simulation and experimental results proves the accuracy of the proposed observer. Only the proposed algorithm and the research in (Cordero et. al., 2017) explores the use of a type-III angle tracking observer for resolver.

In this paper, it is not considered the effect of phase or amplitude mismatch in the resolver signals. These problems are the main source of uncertainties in the angle estimation. For example, considering a RDC with a resolution of 12 bits, an amplitude mismatch of 0.3% in the resolver output signals produce an error of 1 LSB (Szymczak et. al., 2014). However, it is possible to applied compensation algorithms to attenuate the mismatches in resolver signals (Bergas-Jané et. al., 2012; Noori and Khaburi, 2016).

2 Resolver Sensor

2.1 Resolver

Resolver can be modeled as a two-phase machine with an excitation rotor winding (coupled to the motor shaft) and two output stator windings, according to Fig. 1. The excitation winding receive a high-frequency sinusoidal excitation voltage $v_e(t)$ (Idkhajine et. al., 2012):

$$v_e(t) = a_e \cos(2\pi f_e t) \quad (1)$$

where a_e is the excitation amplitude, f_e is the excitation frequency (1 to 10 kHz) and t denotes time. The excitation voltage and the movement of the excitation winding produce two amplitude-modulated signals ($v_s(t)$ and $v_c(t)$) in the output windings:

$$v_s(t) = k_e a_e \cos(2\pi f_e t) \sin(\theta) \quad (2)$$

$$v_c(t) = k_e a_e \cos(2\pi f_e t) \cos(\theta) \quad (3)$$

Equations (2) and (3) indicate that the resolver outputs are amplitude modulated signals. Phase or amplitude mismatch in the resolver signals create uncertainties in the angle estimation. For example, considering a RDC with a resolution of 12 bits, an amplitude mismatch of 0.3% in the resolver output signals produces an error of 1 LSB (Szymczak et. al., 2014).

2.2 Synchronous Demodulation

Synchronous demodulation is a simple technique to estimate the sine and cosine of the angular position from resolver outputs, as shown in Fig. 2. Data acquisition system is synchronized with the resolver excitation signal so that resolver outputs are sampled at the peaks and/or valleys of the resolver excitation signal, i.e., when $\cos(2\pi f_e t) = 1$ and/or $\cos(2\pi f_e t) = -1$. Thus, according to (1), (2) and (3), we have:

$$v_s(t) = \begin{cases} k_e a_e \sin(\theta); & v_e(t) = a_e \\ -k_e a_e \sin(\theta); & v_e(t) = -a_e \end{cases} \quad (4)$$

$$v_c(t) = \begin{cases} k_e a_e \cos(\theta); & v_e(t) = a_e \\ -k_e a_e \cos(\theta); & v_e(t) = -a_e \end{cases} \quad (5)$$

Note that synchronous demodulation is an under-sampling technique. Due to the excitation signal is generated by the same digital processor used to estimate the angular position, synchronous demodulation is possible to implement in a digital processor.

3 Proposed Approach

Fig. 3 shows the proposed approach. It is composed by the synchronous demodulators and the type-III angle tracking observer (ATO). The integrators (1/s) are implemented using Backward Euler discretization. In this paper, amplitude or phase mismatches are not considered, due to the objective of this paper is to develop an improved ATO. Compensation algorithms such the proposed in (Bergas-Jané et. al., 2011; Noori and Khaburi, 2016) can be used to compensate mismatch effects.

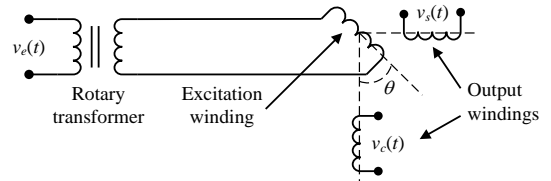
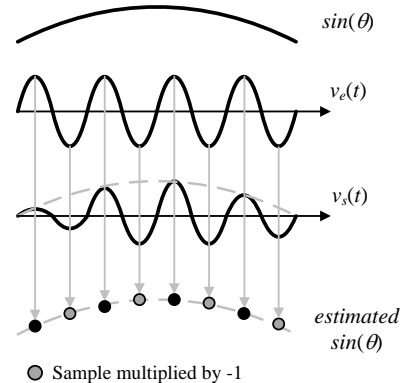


Figure 1. Scheme of the resolver angular position sensor.



● Sample multiplied by -1

Figure 2. Synchronous sampling of the resolver output signals.

3.1 Synchronous Demodulator

Synchronous demodulation takes samples at both the peaks and the valleys of the resolver excitation, as illustrated in Fig. 4. The square wave represents the sampling instants. It is synchronized with $v_e(t)$, so that their positive and negative transitions happen at the peaks and valleys of $v_e(t)$, respectively. If the samples are acquired when the resolver excitation signal is negative, then the samples are multiplied by -1, according to (4) and (5). Thus, the demodulators give the signals d_s and d_c :

$$d_s = k_e a_e \sin(\theta) \quad (6)$$

$$d_c = k_e a_e \cos(\theta) \quad (7)$$

Observe that, using both the peaks and valleys of $v_e(t)$, the sampling frequency of the resolver signals are twice the excitation frequency.

$$f_s = 2f_e \quad (8)$$

If only the peaks or valleys were used, the sampling frequency would be equal to f_e .

3.2 Angle Tracking Observer

Fig. 3 shows the angle tracking observer (ATO) used in this research, which is based on (Cordero et. al., 2017), but using synchronous demodulation. The signal g_e is calculated as follows:

$$\begin{aligned} g_e &= k_e a_e \sin(\theta) \cos(\theta_e) - \\ & k_e a_e \cos(\theta) \sin(\theta_e) \\ &= k_e a_e [\sin(\theta) \cos(\theta_e) - \cos(\theta) \sin(\theta_e)] \\ &= k_e a_e \sin(\theta - \theta_e) \\ &\approx k_e a_e (\theta - \theta_e) \end{aligned} \quad (9)$$

Equation (9) shows that g_e is proportional to the estimation error $e_\theta = \theta - \theta_e$. On the other hand, in the oversampling technique (Cordero et. al., 2017), the same signal g_e is obtained as follows:

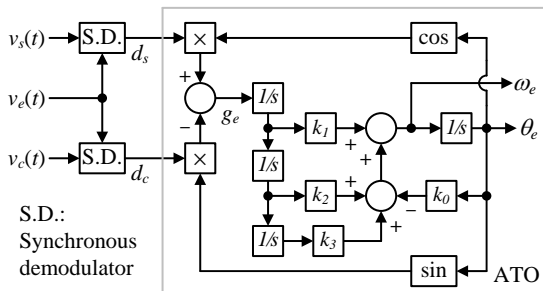


Figure 3. Proposed Observer.

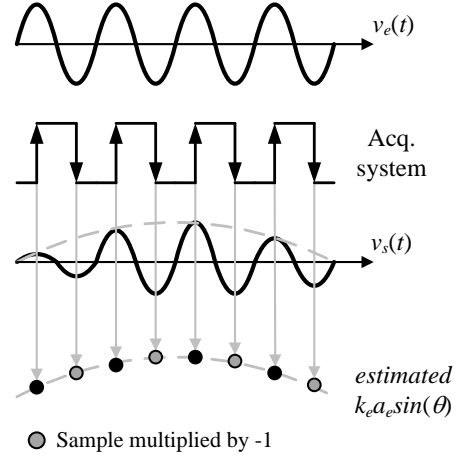


Figure 4. Proposed synchronous demodulator.

$$\begin{aligned} g_e &= v_e(t)[v_s(t) \cos(\theta_e) - v_c(t) \sin(\theta_e)] \\ &= k_e v_e^2 [\sin(\theta) \cos(\theta_e) - \cos(\theta) \sin(\theta_e)] \\ &= k_e v_e^2 \sin(\theta - \theta_e) \\ &\approx 0.5 k_e a_e^2 [1 + \cos(4\pi f_e t)] (\theta - \theta_e) \end{aligned} \quad (10)$$

In (10), g_e is composed by two signals: a low-frequency signal proportional to $e_\theta = \theta - \theta_e$, and a high-frequency signal proportional to $e_\theta \cos(4\pi f_e t)$. It is necessary a low-pass filter (the observer can also act as a filter) to remove the high-frequency signal, in order to g_e be proportional to the angle estimation error, as in (9). For that reason, many samples of the resolver signals must be acquired for the filtering process, and high sampling frequencies are needed.

Based on (9), the ATO in Fig. 3 can be redesigned as in Fig. 5. Note that the ATO is a type-III system, capable to track even parabolic reference signals. Due to the reference and the output signal of the ATO is the angular position, a constant waveform represents a constant position ($\theta = k$), a linear waveform corresponds to a constant speed ($\theta = \omega t$), while a parabolic waveform corresponds to constant acceleration ($\theta = at^2$).

From Fig. 5, and based on (Bishop and Dorf, 1998; Cordero et. al., 2017), the closed-loop space state model of the ATO is described as follows:

$$\dot{\mathbf{E}} = (\mathbf{A} - \mathbf{BK})\mathbf{E} \quad (11)$$

where \mathbf{E} is the error vector and:

$$\begin{aligned} \mathbf{A} &= \begin{bmatrix} 0 & 0 & 0 & 0 \\ -1 & 0 & 0 & 0 \\ 0 & 1 & 0 & 0 \\ 0 & 0 & 1 & 0 \end{bmatrix}; \quad \mathbf{B} = \begin{bmatrix} k_r a_r \\ 0 \\ 0 \\ 0 \end{bmatrix} \\ \mathbf{K} &= [k_0 \quad -k_1 \quad -k_2 \quad -k_3] \end{aligned} \quad (12)$$

It is possible to use linear control techniques such as Ackermann formula or linear matrix inequalities (LMI) to set the poles of (11) and adjust the dynamics of the ATO. The integrators in Fig. 3 are implemented using Backward Euler discretization.

$$\frac{1}{s} = \frac{t_s \cdot z}{z-1}; \quad t_s = \frac{1}{f_s} \quad (13)$$

3 Results

The proposed angle tracking observer with synchronous demodulation was simulated in MATLAB/SIMULINK. The parameters of the resolver sensor and the gains are listed in Table 1. The poles of the ATO were set in $-40+j40$, $-40-j40$, -35 and -35 . The gains of the ATO were set through Ackermann formula.

The sampling frequency used in synchronous demodulation and in the discrete integrators is 10 kHz, which is 5 times less than the sampling frequency in (Cordero et. al., 2017). In (Bergas-Jané et. al., 2012), the sampling frequency is 288 kHz.

The mechanical speed used in the simulation is shown in Fig. 6: a constant acceleration from 0 to 100 rad/s in 1s, and a constant speed of 100 rad/s.

Fig. 7 shows the synchronous demodulation for $v_s(t)$. The demodulated signal is a good estimative of the envelope of the resolver output. The angle estimation error is shown in Fig. 8. The steady-state error tends to zero, even for constant acceleration. This result is due to the ATO is a type-III system.

In order to test the proposed observer, white noise (zero mean, variance 0.0002) was added to the resolver outputs. Figs. 9 and 10 show the simulation results. The steady-state error of the angle estimation is less than 0.0044 rad, which is the typical error in industrial applications (Ellis, 2004).

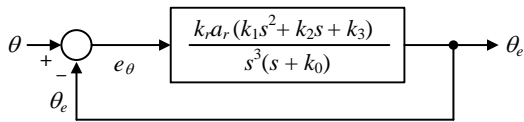


Figure 5. Simplified structure of the ATO.

Table 1. Parameters of the Resolver and the Angle Observer.

Parameter	Value
a_e	1
k_e	1
f_e	5 kHz
k_0	150
k_1	10025
k_2	322000
k_3	3920000
$f_s = 2 \cdot f_e$	10 kHz ($t_s = 0.1$ ms)

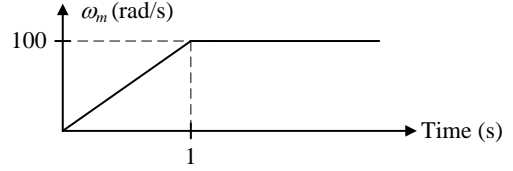


Figure 6. Speed curve used in simulation.

The proposed RDC algorithm was experimentally implemented in the DSP DSPACE DS1104. Following the strategy explained in (Sarma et.al., 2008), the DSP was also used to generate the resolver signals. This strategy allows defining the angular position used in the test, in order to make an adequate comparison between the real and the estimated angle (the angular position is known in each instant of time). Besides, it is possible to test the robustness of the proposed RDC algorithm by adding noise to the resolver signals.

The resolver signals were generated using a sampling frequency of 50 kHz. The sampling frequency used in the synchronous demodulation and for the discrete integrators in the ATO was set in 10 kHz, which is 5 times less than the switching frequency used in (Cordero et. al., 2017). The experimental setup is shown in Fig. 11. The digital-to-analog converters (DACs) of the DSP were used to show the experimental results.

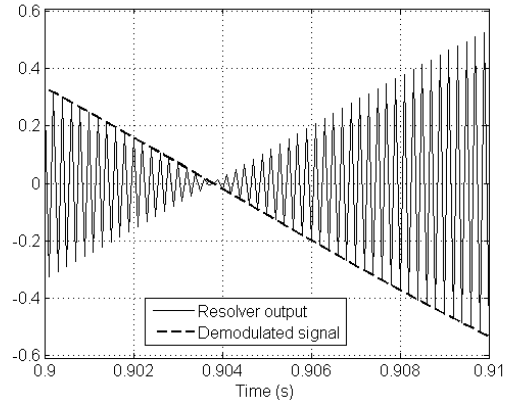


Figure 7. Simulation result for synchronous demodulation.

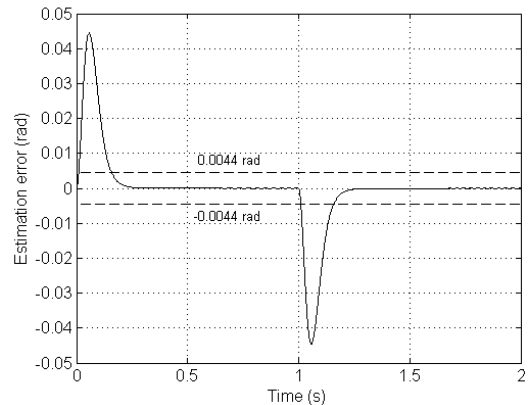


Figure 8. Simulation result for angle estimation error.

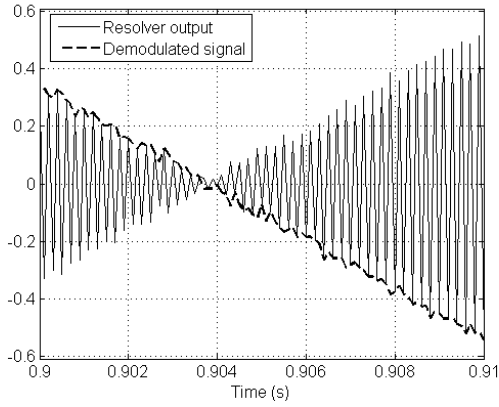


Figure 9. Simulation result for synchronous demodulation with noise.

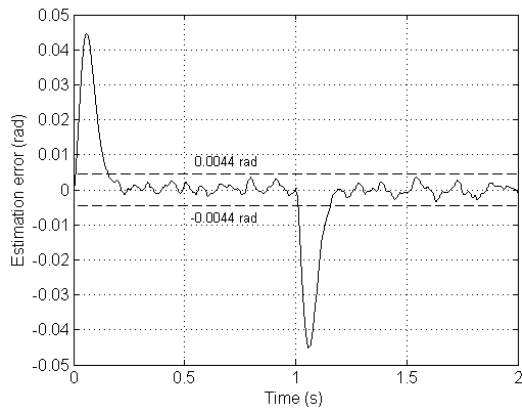


Figure 10. Simulation result for angle estimation error with noise.

Figs. 12 and 13 show the experimental results for the demodulation process and the angle estimation error without noise. Due to the angle estimation error is small, it was necessary to amplify this error signal before sending it to the DSP DACs. Thus, the vertical scale of Fig. 13 was 50V/rad. Then, the maximum angle estimation error is $2.28/50 = 0.0456$ rad, which is similar than the maximum error peak in Fig. 10.

Fig 14 shows the experimental result for angle estimation adding the same noise (zero mean, variance 0.0002) than in the simulations. The experimental steady-state error is a bit greater than the values obtained in simulations, but it is still less than ± 0.044 rad. It is important to observe than some electromagnetic interference is added to the measurements, so the estimation error actually is less than the values shown in Fig. 13 and 14.



Figure 11. Experimental setup using the DSP DSPSPACE DS1104

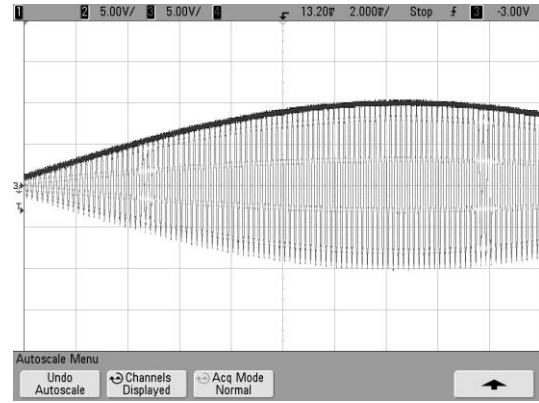


Figure 12. Experimental result for synchronous demodulation.

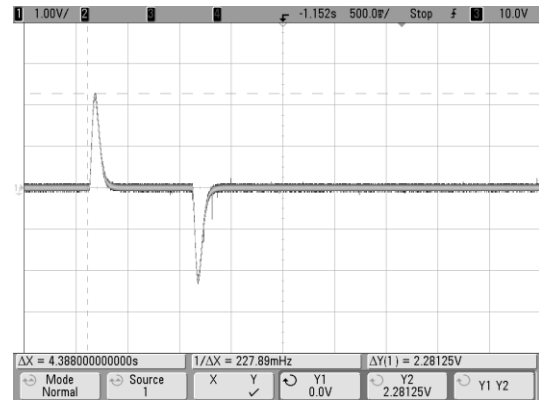


Figure 13. Experimental result for angle estimation error. Vertical scale: 50V/rad.

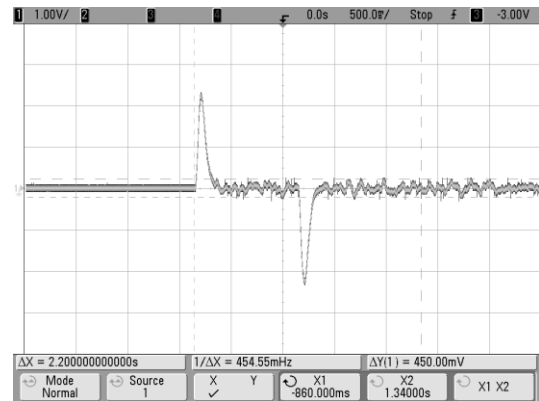


Figure 14. Experimental result for angle estimation error with noise. Vertical scale: 50V/rad.

4 Conclusion

This paper proposes the use of synchronous demodulation of the resolver output signals with the tracking capabilities of a type-III angle tracking observer. The synchronous demodulation allows working with low sampling frequencies, without losing accuracy, which reduces the computational cost of the algorithm. The steady-state angle estimation error is small, even when noise is added. Thus, the proposed algorithm

has accuracy, robustness against noise and easy to implement using a low sampling frequency.

Acknowledgment

Authors want to thanks BATLAB laboratory - UFMS for the support to this research.

References

- Bergas-Jané, J., Ferrater-Simón, C., Gross, G., Ramírez-Pisco, R., Galceran-Arellano, S. and Rull-Duran, J. (2012). High-Accuracy All-Digital Resolver-to-Digital Conversion. *IEEE Transactions on Industrial Electronics*, vol. 59, no. 1, pp. 326–333.
- Carusso, M. di Tomasso, A. O., F. Genduso, F., Miceli, R. and Galluzzo, G. R. (2016). A DSP-Based Resolver-to-Digital Converter for High Performance Electrical Drive Applications. *IEEE Transactions on Industrial Electronics*, Vol. 63, No. 7, pp. 4042–4051.
- Cordero, R., Pinto, J. O. P., Suemitsu, W. I. and Soares, J. O. (2017). Improved Demultiplexing Algorithm for Hardware Simplification of Sensored Vector Control Through Frequency-Domain Multiplexing. *IEEE Transactions on Industrial Electronics*, Vol. 64, No. 8, pp. 6583–6548.
- Dorf, R. C. and Bishop, R. H. (1998). *Modern Control Systems*, 8th ed., Addison Wesley, pp. 415-665.
- Ellis, G. (2004), *Control System Design Guide*, 3rd ed., Elsevier, pp. 278–292.
- Idkhajine, L., Monmasson, E., Naouar, M. W., Prata, A. and Boullaga, K. (2009). Fully Integrated FPGA-based Controller for Synchronous Motor Drive. *IEEE Transactions on Industrial Electronics*, Vol. 56, No. 10, pp. 4006–4017.
- Jin, C.-S., Jang, I.-S., Bae, J.-N., Lee, J. and Kim, W.-H. (2015). Proposal of Improved Winding Method for VR Resolver. *IEEE Transactions on Magnetics*, Vol. 51, No. 3, pp. 1–4.
- Kaewjinda, W. and Konghirun, M. (2006). A DSP – Based Vector Control of PMSM Servo Drive Using Resolver Sensor. *IEEE Region 10 Conference*, pp. 1–4.
- Noori, N. and Khaburi, D. A. (2016). Diagnosis and compensation of amplitude imbalance, imperfect quadrant and offset in resolver signals. *7th Power Electronics and Drive Systems Technologies Conference*, pp. 76–81.
- Qamar, N. A., Hatziaioniu, C. J. and Wang, H. (2015). Speed Error Mitigation for a DSP-Based Resolver-to-Digital Converter Using Autotuning Filters. *IEEE Trans. Ind. Electron.*, Vol. 62, No. 2, pp. 1134–1139.
- Sarma, S., Agrawal, V. K. and S. Udupa, S. (2008). Software-based Resolver-To-Digital Conversion Using a DSP. *IEEE Transactions on Industrial Electronics*, Vol. 55, No. 1, pp. 371–379.
- Staebler, M. and Verma, A., 2017. TMS320F240 DSP Solution for Obtaining Resolver Angular Position and Speed, Texas Instruments Application Report SPRA605A.
- Szymczak, J., O’Meara, S., Gealon, J. S. and De La Rama, C. N. (2014). Precision Resolver-to-Digital Converter Measures Angular Position and Velocity. *ANALOG Devices – ANALOG DIALOGUE*, Vol. 48, No. 3, pp. 1–6.
- Wang, W Y., Zhu, Z. and Zuo, Z. (2015). A Novel Design Method for Resolver-to-Digital Conversion. *IEEE Transactions on Industrial Electronics*, Vol. 62, No. 6, pp. 3724–3731.
- Zhang, Z., Ni, F., Dong, Y., Guo, C., Jin, M. and Liu, H. (2015). A Novel Absolute Magnetic Rotary Sensor. *IEEE Transactions on Industrial Electronics*, Vol. 62, No. 7, pp. 4408–4419.